

Disodium *cis*-1,2-dicyano-1,2-ethylenedithiolate and the metal complexes were prepared by published methods.¹⁹ Far-infrared spectra were measured on a Hitachi Perkin-Elmer FIS 3 spectrometer. The samples were ground dry and then made into a mull with Vaseline. The mull was smoothed onto a polyethylene plate which was mounted in the sample beam. Electronic spectra were obtained on a Cary 14 spectrometer with solution samples in 1-cm cells. Peak positions are observed maxima with no line fitting. Melting points on a Fisher-Johns apparatus are uncorrected.

Bis(2-propanethiolato)bis(triphenylphosphine)platinum(II), Pt(2-PrS)₂(PPh₃)₂. To a suspension of *cis*-PtCl₂(PPh₃)₂ (208 mg) in dichloromethane (10 mL) was added 2-propanethiol (0.1 mL) and triethylamine (0.1 mL). Immediately the reaction mixture changed color, and a yellow solution was obtained. The solution was filtered to remove any precipitated Et₃N·HCl, and the volume of the solution reduced to 3-4 mL on a rotary evaporator. Diethyl ether was slowly added to the solution when the complex precipitated. The yellow compound was filtered, washed sequentially with water (to remove any remaining Et₃N·HCl), ethanol, and diethyl ether, and dried in vacuo: yield 115 mg (50%); mp 129-131 °C. Anal. Calcd for C₄₂H₄₄P₂PtS₂: C, 58.0; H, 5.10; S, 7.37. Found: C, 58.2; H, 5.39; S, 7.46. As an alternative to using triethylamine, we have used hydroxide washed Dowex I-8 ion-exchange resin. The reaction proceeds more slowly, but high purity product is obtained. The complex can be recrystallized by dissolution in the minimum volume of chloroform followed by the slow addition of the solution to diethyl ether. ¹H NMR data: δ 1.34 (CH₃, ³J = 7 Hz), δ 4.21 (CH, m).

Bis(2-propanethiolato)bis(triphenylarsine)platinum(II), Pt(2-PrS)₂(AsPh₃)₂. With an analogous procedure, the triphenylarsine complex was prepared; mp 102-104 °C. Anal. Calcd for C₄₂H₄₄As₂PtS₂: C, 52.7; H, 4.63. Found: C, 52.8; H, 5.01.

Bis[bis(2-propanethiolato)bis(triphenylphosphine)platinum(II)]nickel(II) Perchlorate, [[Pt(2-PrS)₂(PPh₃)₂]₂Ni](ClO₄)₂. To a solution of Pt(2-PrS)₂(PPh₃)₂ (189 mg) in dichloromethane (5 mL) was added nickel perchlorate [Ni(H₂O)₆](ClO₄)₂ (74 mg) in acetonitrile (5 mL). The color of the solution changed from yellow to blue. The volume was reduced to 1-2 mL on a rotary evaporator. Ethanol (~1 mL) was added, and then diethyl ether was slowly added until the complex began to precipitate. The complex was filtered, washed with diethyl ether, and dried in vacuo; yield 182 mg (42%). Anal. Calcd for C₈₄H₈₈Cl₂NiO₈P₄Pt₂S₄: C, 50.5; H, 4.44; S, 6.42. Found: C, 50.2; H, 4.60; S, 6.16. The compound melts with decomposition to a red liquid at 235-240 °C. The compound gives a blue solution in acetonitrile, acetone, and ethanol. ¹H NMR data: δ 1.25 (CH₃, d).

Bis[bis(thiophenolato)bis(triphenylphosphine)platinum(II)]nickel(II) Perchlorate, [[Pt(PhS)₂(PPh₃)₂]₂Ni](ClO₄)₂. To a solution of Pt(PhS)₂(PPh₃)₂ (86 mg) in dichloromethane (5 mL) was added [Ni(H₂O)₆](ClO₄)₂ in acetonitrile (~5 mL). The mixture was stirred for 30 min. The volume of solution was reduced and ethanol (2-3 mL) added. Slow addition of diethyl ether gave the complex as a brown precipitate; yield 43 mg. Anal. Calcd for C₉₆H₈₀Cl₂NiO₈P₄Pt₂S₄: C, 54.0; H, 3.78; S, 6.01. Found: C, 53.4; H, 4.00; S, 5.54.

Bis[bis(thiophenolato)[1,2-bis(diphenylphosphino)ethane]palladium(II)]nickel(II) Perchlorate, [[Pd(PhS)₂dppe]₂Ni](ClO₄)₂. With a similar procedure the complex was obtained as brown crystals. Anal. Calcd for C₇₆H₆₈Cl₂NiO₈Pd₂P₄S₄: C, 53.6; H, 4.02. Found: C, 53.1; H, 4.20.

Bis[bis(thiophenolato)[1,2-bis(diphenylphosphino)ethane]nickel(II)]nickel(II) Perchlorate, [[Ni(PhS)₂dppe]₂Ni](ClO₄)₂. Again by use of a similar procedure the complex was obtained as a red-brown solid. Anal. Calcd for C₇₆H₆₈Cl₂Ni₂O₈P₄S₄: C, 56.7; H, 4.26; S, 7.97. Found: C, 55.8; H, 4.07; S, 8.38.

(1,4,8,11-Tetrathiaundecanato)palladium(II), Pd(TTU). To a solution of 1,4,8,11-tetrathiaundecane (TTU) (438 mg) in ethyl acetate (~10 mL) was added a suspension of palladium acetate (401 mg) in ethyl acetate (~10 mL). A yellow precipitate formed. After the solution was stirred for 2 h, the solid was filtered, washed with diethyl ether, and dried in vacuo: yield quantitative; mp 200-205 °C dec. Anal. Calcd for C₇H₁₄PdS₄: C, 25.3; H, 4.24. Found: C, 25.2; H, 4.21. The complex can be purified by dissolution in the minimum volume of chloroform, followed by precipitation with a small quantity

of ethanol followed by diethyl ether.

Bis[(1,4,8,11-tetrathiaundecanato)palladium(II)]nickel(II) Perchlorate, [[Pd(TTU)₂Ni](ClO₄)₂. To a solution of Pd(TTU) (238 mg) in chloroform (15 mL) was added a solution of nickel perchlorate (251 mg) in acetonitrile (6 mL). The reaction mixture was stirred for up to 12 h. To the mixture was added diethyl ether (20 mL) and the precipitate filtered, washed with diethyl ether, and dried in vacuo; yield quantitative. Anal. Calcd for C₁₄H₂₈Cl₂NiO₈Pd₂S₈: C, 18.2; H, 3.06. Found: C, 17.6; H, 2.92.

Bis(1,4,8,11-tetrathiaundecanato)zinc Acetate, [Zn₂(TTU)₂(OAc)₂. To a stirred suspension of zinc acetate in acetone solvent was added excess TTU. A white precipitate immediately formed. The precipitate was sequentially washed with water, ethanol, and then diethyl ether and dried in vacuo. Anal. Calcd for C₁₈H₃₄O₄S₄Zn: C, 28.2; H, 4.47. Found: C, 28.6; H, 4.56. IR spectrum shows ν(CH₃CO₂⁻) at 1540 cm⁻¹.

[Bis(1,4,8,11-tetrathiaundecanato)trinickel] Tetracyanoquinodimethane, [Ni₃(TTU)₂](TCNQ)₂. The complex was prepared as an insoluble dark precipitate by mixing acetonitrile solutions of [Ni₃(TTU)₂](BF₄)₂ and Li⁺ TCNQ⁻ in a mole ratio of 1:2. The product was washed with acetonitrile and then diethyl ether and dried in vacuo. Anal. Calcd for C₃₈H₃₆Ni₃N₄S₈: C, 44.0; H, 3.49; N, 10.8; S, 24.7. Found: C, 43.9; H, 3.76; N, 10.6; S, 24.2.

Acknowledgment. I sincerely thank Dr. Robert Somoano of the Jet Propulsion Laboratory in Pasadena, California, for carrying out the compacted powder conductivity measurements.

Registry No. Pt(2-PrS)₂(PPh₃)₂, 72137-83-8; Pt(2-PrS)₂(AsPh₃)₂, 72137-84-9; [[Pt(2-PrS)₂(PPh₃)₂]₂Ni](ClO₄)₂, 72137-86-1; [[Pt(PhS)₂(PPh₃)₂]₂Ni](ClO₄)₂, 72137-88-3; [[Pd(PhS)₂dppe]₂Ni](ClO₄)₂, 72137-90-7; [[Ni(PhS)₂dppe]₂Ni](ClO₄)₂, 72137-92-9; Pd(TTU), 72137-93-0; [[Pd(TTU)₂Ni](ClO₄)₂, 72137-95-2; [Zn₂(TTU)₂](OAc)₂, 72137-97-4; [Ni₃(TTU)₂](TCNQ)₂, 72173-17-2; [Ni₃(TTU)₂](BF₄)₂, 59738-24-8; Pt(PhS)₂(PPh₃)₂, 72173-18-3; [Pt(PhS)₂]_n, 59738-65-7; Pt(PhS)₂(PMe₂Ph)₂, 72173-19-4; Pt(PhS)₂(diars), 59765-76-3; Pt(SCH₂CH₂S)(PPh₃)₂, 56213-51-5; Pt(PhS)₂(AsPh₃)₂, 72137-98-5; [Pd(PhS)₂]_n, 59738-64-6; Pd(PhS)₂(PMe₂Ph)₂, 59738-10-2; Pd(PhS)₂(diars), 59738-11-3; Pd(PhS)₂(dppe), 33971-07-2; [Pd(SCH₂CH₂S)(PPh₃)₂, 56213-52-6; Ni(SCH₂CH₂S)dppe, 56213-47-9; Ni(PhS)₂dppe, 62637-81-4; Pd(SCH₂CH₂S)dppe, 72138-04-6; [Ni₃(SCH₂CH₂NH₂)₄Cl₂, 29993-19-9; [Ni₃(SCH₂CH₂NH₂)₄](TCNQ)₂, 72173-20-7; [Ni₃(SCH₂CH₂NH₂)₄]-[Ni(S₂C₂(CN)₂)₂], 72173-21-8; [Ni₃(TTU)₂][Ni(S₂C₂(CN)₂)₂], 72173-22-9; [Ni₃(TTU)₂][Co(S₂C₂(CN)₂)₂], 72173-23-0; [Ni₃(TTU)₂][Fe(S₂C₂(CN)₂)₂], 72173-24-1; *cis*-PtCl₂(PPh₃)₂, 15604-36-1.

Contribution from the Guelph-Waterloo Centre,
Waterloo Campus, Department of Chemistry,
University of Waterloo, Waterloo, Ontario, Canada N2L 3G1

Binuclear Metal Carbonyls: Molecular Structure of μ -Chloro- μ -(diphenylphosphido)-hexacarbonyldiiron (Fe-Fe)

Nicholas J. Taylor, Graham N. Mott, and Arthur J. Carty*

Received June 5, 1979

We recently described a synthetic route to the halo-bridged binuclear iron carbonyls Fe₂(CO)₆(X)(PPh₂) (X = Cl, Br, I).¹ These compounds are potentially useful reagents for generating coordinatively unsaturated binuclear iron fragments via treatment with soluble silver salts and precipitation of silver halide. The chloro complex Fe₂(CO)₆(Cl)(PPh₂) is the first chloro-bridged iron carbonyl to be described, and we report herein details of the crystal and molecular structure.

(18) Melby, L. R.; Harder, R. J.; Hertler, W. R.; Mahler, W.; Benson, R. E.; Mochel, W. E. *J. Am. Chem. Soc.* **1962**, *84*, 3374.

(19) Davison, A.; Holm, R. H. *Inorg. Synth.* **1967**, *10*, 8.

(1) Mott, G. N.; Carty, A. J. *Inorg. Chem.* **1979**, *18*, 2926.

Experimental Section

Collection and Reduction of X-ray Data. As initially prepared¹ Fe₂(CO)₆(Cl)(PPh₂) is an oil. A sample which had been sublimed onto a cold finger at 10⁻⁴ mm gradually crystallized on standing over a 3-month period. Recrystallization from petroleum ether afforded red-brown prisms. Preliminary X-ray examination established a four molecule orthorhombic unit cell with systematic absences hkl , $h + k = 2n + 1$, and $h0l$, $l = 2n + 1$, consistent with the choice of space groups $Cmc2_1$, $C2cm$ (nonstandard setting for $Ama2$), or $Cmcm$. Solution and refinement of the structure confirmed the choice as $Cmc2_1$. Least-squares refinement of the setting angles of 15 reflections for which $24^\circ < 2\theta < 34^\circ$ gave the cell constants $a = 10.560$ (3) Å, $b = 12.604$ (2) Å, $c = 14.928$ (3) Å, $V = 1986.8$ (8) Å³, $M = 500.40$, $\rho_{\text{calcd}} = 1.673$ g·cm⁻³, $\rho_{\text{measd}} = 1.68$ g·cm⁻³, $Z = 4$, and $F(000) = 1000$.

Intensity data were collected on a Syntex P2₁ instrument with graphite-monochromated Mo K α radiation ($K\alpha_1$, $\lambda = 0.70926$ Å; $K\alpha_2$, $\lambda = 0.71354$ Å). Crystal dimensions were $0.22 \times 0.27 \times 0.28$ mm. The temperature was constant at 22 (1) °C. A θ - 2θ scan mode with variable scan speed of 2.0–29.3°/min in 2θ was used. The scan width was from $[2\theta(\text{Mo } K\alpha_1) - 1.0]^\circ$ to $[2\theta(\text{Mo } K\alpha_2) + 1.0]^\circ$. Background measurements were made at the beginning and end of each scan, each measurement for one-fourth of the scan time. Two standard reflections 440 and 404 were measured after every 98 reflections to check stability and crystal decay. No significant change in intensity was noted over the course of data collection. Of the 1584 symmetry independent reflections measured ($3^\circ \leq 2\theta \leq 60^\circ$), all those with intensities $I \geq 3\sigma(I)$ (1261) were used in subsequent calculations. Standard deviations were estimated from counting statistics. Data were reduced to unscaled, observed structure factor amplitudes after correction for Lorentz and polarization factors. With $\mu = 17.43$ cm⁻¹, no absorption correction was deemed necessary.

Solution and Refinement of the Structure. Among the indicated choices of space groups, $Cmc2_1$ requires that the molecule should straddle a mirror plane through the expected bridging chlorine atom and also bisect the bridging diphenylphosphido group. With $C2cm$, either twofold or mirror symmetry is required for $Z = 4$. The centrosymmetric option $Cmcm$ would require the unlikely situation of either mm or $2/m$ symmetry imposed on the molecule.

From a Patterson synthesis, it was immediately obvious that the correct choice of space group was $Cmc2_1$ (C_{2v}^{12} , No. 36). The Patterson was solved for the iron, phosphorus, and chlorine atoms (although at this stage, it was impossible to differentiate between Cl and P). A Fourier synthesis, with phases derived from a least-squares refinement of the aforementioned atoms, was used to determine the positions of the remaining nonhydrogen atoms. The phenyl rings of the diphenylphosphido group were somewhat difficult to resolve at this stage. One phenyl ring was found to be bisected by the mirror plane while the other was coplanar with the mirror plane.

With all atoms having isotropic thermal parameters, the structure was refined to an R factor ($R = \sum[|F_o| - |F_c|] / \sum|F_o|$) of 0.075. Conversion to anisotropic thermal parameters reduced R to 0.042. At this stage, a difference Fourier synthesis was utilized to determine the position of all hydrogen atoms. Inclusion of these atoms in the refinement gave convergence at $R = 0.030$. R_w , the weighted residual ($R_w = \{\sum w[|F_o| - |F_c|]^2 / \sum w|F_o|^2\}^{1/2}$), was 0.042 ($w^{-1} = 2.6 - 0.05|F_o| + 0.0004|F_o|^2$). Maximum residual electron density of 0.25 e Å⁻³ was located in the vicinity of the iron-iron bond. Although this model (A) was satisfactory, in terms of the residuals R and R_w and also chemically reasonable, it was subsequently realized that despite the presence of a plane of symmetry bisecting the molecule the crystal itself was chiral. Accordingly, in an attempt to establish the handedness of the crystal a rerefinement was carried out under identical conditions but with the coordinates along the polar c axis reversed (i.e., $x, y, z \rightarrow x, y, -z$). Convergence (model B) was achieved at $R = 0.028$ and $R_w = 0.030$. According to Hamilton's R factor test² using the weighted residuals R_w , we can reject the hypothesis that the first model refined (A) has the correct absolute configuration at a confidence level better than 0.005. The correct absolute configuration is therefore that given by the second model B. Positions, bond lengths, and angles in Tables I and II correspond to this absolute configuration. In fact a comparison of bond lengths and angles for the two models would not permit an unequivocal assignment of chirality. Indeed the only differences of significance are in the Fe-Cl bond length (2.289

Table I

Atomic Positional Parameters (Fractional, $\times 10^4$) for Fe₂(CO)₆(Cl)(PPh₂)

	x	y	z
Fe	1212.5 (4)	304.3 (3)	0
Cl	0	716 (1)	1222 (1)
P	0	-1147.5 (8)	93.9 (9)
O(1)	1668 (4)	2582 (2)	-340 (3)
O(2)	3562 (3)	-285 (3)	920 (3)
O(3)	2087 (4)	-167 (3)	-1805 (3)
C(1)	1485 (4)	1708 (3)	-213 (3)
C(2)	2653 (4)	-65 (4)	557 (3)
C(3)	1720 (4)	1 (3)	-1102 (3)
C(11)	0	-1849 (4)	1168 (3)
C(12)	1124 (4)	-2138 (4)	1571 (3)
C(13)	1121 (6)	-2717 (4)	2361 (4)
C(14)	0	-3003 (6)	2745 (5)
C(21)	0	-2232 (4)	-713 (3)
C(22)	0	-3293 (4)	-432 (4)
C(23)	0	-4113 (4)	-1046 (4)
C(24)	0	-3918 (4)	-1943 (4)
C(25)	0	-2874 (5)	-2247 (4)
C(26)	0	-2048 (4)	-1633 (4)

Hydrogen Atom Coordinates (Fractional, $\times 10^3$) and B_{iso} (Å²)

	x	y	z	B
H(12)	189 (4)	-197 (3)	133 (3)	4.6 (8)
H(13)	194 (5)	-283 (4)	260 (2)	5.7 (9)
H(14)	0	-338 (6)	332 (5)	5 (1)
H(22)	0	-341 (4)	13 (4)	4 (1)
H(23)	0	-478 (5)	-82 (5)	5 (2)
H(24)	0	-445 (5)	-242 (5)	6 (2)
H(25)	0	-270 (4)	-281 (4)	4 (1)
H(26)	0	-134 (4)	-189 (4)	3 (1)

Table II. Bond Lengths (Å) and Angles (Deg) for Fe₂(CO)₆(Cl)(PPh₂)

(a) Bond Lengths			
Fe-Fe'	2.5607 (5)	P-C(21)	1.822 (5)
Fe-Cl	2.289 (1)	C(11)-C(12)	1.380 (5)
Fe-P	2.238 (1)	C(12)-C(13)	1.386 (7)
Fe-C(1)	1.821 (3)	C(13)-C(14)	1.364 (7)
Fe-C(2)	1.795 (4)	C(21)-C(22)	1.402 (7)
Fe-C(3)	1.772 (4)	C(22)-C(23)	1.381 (8)
C(1)-O(1)	1.134 (5)	C(23)-C(24)	1.361 (9)
C(2)-O(2)	1.137 (6)	C(24)-C(25)	1.392 (8)
C(3)-O(3)	1.138 (6)	C(25)-C(26)	1.387 (8)
P-C(11)	1.831 (5)	C(26)-C(21)	1.393 (7)
(b) Angles			
Fe'-Fe-Cl	56.0 (0)	Fe-P-C(21)	124.9 (1)
Fe'-Fe-P	55.1 (0)	C(11)-P-C(21)	102.5 (1)
Fe'-Fe-C(1)	99.1 (1)	Fe-C(1)-O(1)	179.1 (1)
Fe'-Fe-C(2)	147.9 (1)	Fe-C(2)-O(2)	178.9 (2)
Fe'-Fe-C(3)	107.6 (1)	Fe-C(3)-O(3)	177.2 (2)
Cl-Fe-P	79.4 (0)	P-C(11)-C(12)	120.6 (1)
Cl-Fe-C(1)	90.4 (1)	C(12)-C(11)-C(12)'	118.7 (2)
Cl-Fe-C(2)	99.4 (1)	C(11)-C(12)-C(13)	120.5 (2)
Cl-Fe-C(3)	163.4 (1)	C(12)-C(13)-C(14)	119.9 (3)
P-Fe-C(1)	153.6 (1)	C(13)-C(14)-C(13)'	120.4 (3)
P-Fe-C(2)	104.1 (1)	P-C(21)-C(22)	121.2 (1)
P-Fe-C(3)	93.1 (1)	P-C(21)-C(26)	121.8 (1)
C(1)-Fe-C(2)	101.5 (1)	C(26)-C(21)-C(22)	117.0 (2)
C(1)-Fe-C(3)	90.0 (1)	C(21)-C(22)-C(23)	121.0 (2)
C(2)-Fe-C(3)	96.8 (2)	C(22)-C(23)-C(24)	121.2 (2)
Fe-Cl-Fe'	68.0 (0)	C(23)-C(24)-C(25)	119.4 (2)
Fe-P-Fe'	69.8 (0)	C(24)-C(25)-C(26)	119.6 (2)
Fe-P-C(11)	116.7 (1)	C(25)-C(26)-C(21)	121.7 (2)
(c) Carbon-Hydrogen Bond Lengths			
C(12)-H(12)	0.91 (4)	C(23)-H(23)	0.91 (6)
C(13)-H(13)	0.95 (5)	C(24)-H(24)	0.98 (7)
C(14)-H(14)	0.99 (7)	C(25)-H(25)	0.87 (6)
C(22)-H(22)	0.85 (6)	C(26)-H(26)	0.97 (5)

(1) Å (B) vs. 2.317 (1) Å (A)), the Fe-Cl-Fe' angle (68.0 (0)° (B) vs. 67.0° (A)), and to a lesser extent the Fe-C(carbonyl) bond lengths (Fe-C(1), 1.821 (3) vs. 1.816 (4); Fe-C(2), 1.795 (5) vs. 1.814 (5);

(2) Hamilton, W. C. *Acta Crystallogr.* 1965, 18, 502.

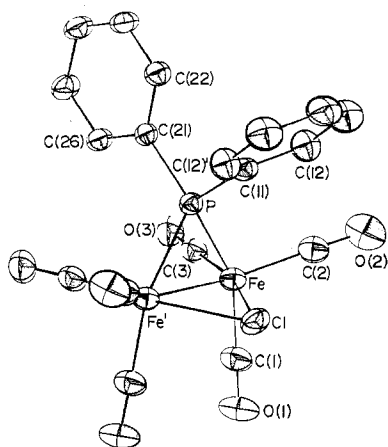


Figure 1. A perspective view of the molecular structure of $\text{Fe}_2(\text{CO})_6(\text{Cl})(\text{PPh}_2)$. Thermal ellipsoids are drawn at the 30% level, and hydrogen atoms are not shown.

$\text{Fe}-\text{C}(3)$, 1.772 (4) vs. 1.738 (5) Å). Scattering factor tables, including the anomalous dispersion correction for iron, were taken from ref 3. Scattering factors for hydrogen were those of ref 4. Anisotropic thermal parameters are included as supplementary data, Table SI, and a list of observed and calculated structure factors is also available.

Results and Discussion

Figure 1 presents a perspective view of the molecule drawn to illustrate the crystallographic mirror plane passing through the phosphorus atom, the midpoint of the $\text{Fe}-\text{Fe}$ bond and the bridging chlorine atom. There are no intermolecular contacts of significance. The central $\text{Fe}_2\text{P}\text{Cl}$ core, which has a butterfly configuration, provides the main structural features of interest. The $\text{Fe}-\text{Fe}'$ bond distance (2.5607 (5) Å) is the shortest and one of the most accurate yet reported for a phosphido-bridged binuclear complex.^{5,6} Thus in $\text{Fe}_2(\text{CO})_6(\text{PPh}_2)_2$ the $\text{Fe}-\text{Fe}$ bond length is 2.623 (3) Å⁵ while in the unsymmetrical derivative $\text{Fe}_2(\text{CO})_6(\text{PPhMe})_2$, which has the shortest $\text{Fe}-\text{Fe}$ bond of any bis(phosphido)-bridged species, the distance is 2.619 (1) Å. Replacement of a bridging diphenylphosphido group by a bridging chloride ligand thus results in a contraction of ~ 0.06 Å in the $\text{Fe}-\text{Fe}$ bond length. This result is not inconsistent with the fact that $\text{Fe}-\text{Fe}$ bond lengths and $\text{Fe}-\text{P}-\text{Fe}$ angles in $\text{Fe}_2(\text{CO})_6(\text{X})_2$ complexes show a general decrease along the series $\text{X} = \text{PR}_2 > \text{SR} > \text{NR}_2$, as the electronegativity of the bridging atom increases and the covalent radius decreases.⁶ The only mixed-bridge complexes for which extensive structural data exist are the zwitterionic hydrocarbyl compounds $\text{Fe}_2(\text{CO})_6\{\text{CHC}(\text{Ph})\text{NRR}'\}(\text{PPh}_2)$ ($\text{R} = \text{c-C}_6\text{H}_{11}$, $\text{R}' = \text{H}$, $\text{Fe}-\text{Fe} = 2.576$ (1) Å⁷; $\text{R} = \text{R}' = \text{Et}$, $\text{Fe}-\text{Fe} = 2.548$ (1) Å⁸), where it is apparent that substitution of PPh_2 in $\text{Fe}_2(\text{CO})_6(\text{PPh}_2)_2$ by the dipolar carbon ligands $\text{C}^-\text{H}-\text{C}^+(\text{Ph})\text{N}^+\text{RR}'$ effects analogous decrements in $\text{Fe}-\text{Fe}$ distances and $\text{Fe}-\text{P}-\text{Fe}$ angles. The $\text{Fe}-\text{P}-\text{Fe}$ angle of 69.8 (0)° is one of the smallest reported to date for a phosphido bridge. Indeed phosphido bridges are remarkably versatile in that they can support a wide range of bonding and nonbonding metal-metal distances. For phosphido-bridged iron complexes the present $\text{Fe}-\text{P}-\text{Fe}$ angle and $\text{Fe}-\text{Fe}$ distance are the lower limits with

angles ranging up to the value of 98.0 (1)° in $\text{Fe}_3(\text{CO})_8[\text{Ph}_2\text{PC}_4(\text{CF}_3)_2]\text{PPh}_2$,⁹ where the $\text{Fe}-\text{Fe}$ distance of 4.59 Å is definitely nonbonding. This demonstrable flexibility of PR_2 bridges may be capable of exploitation in the design of binuclear catalysts where a key feature is the generation and cleavage of metal-metal bonds.

Despite the smaller covalent radius of chlorine (0.99 Å) than of phosphorus (1.10 Å) the $\text{Fe}-\text{Cl}$ bridge bond length 2.289 (1) Å is significantly longer than the $\text{Fe}-\text{P}$ bond length (2.238 (1) Å). We interpret this as a direct reflection of the poor affinity between an iron carbonyl fragment and the chlorine atom as a ligand. Halogeno carbonyls of iron are few in number and, with the exception of the iodides, unstable and difficult to prepare.¹⁰ It is also notable that the $\text{Fe}-\text{C}(3)$ distance (trans to Cl) of 1.772 (4) Å is distinctly shorter than the $\text{Fe}-\text{C}$ bond lengths to carbonyls trans to the $\text{Fe}-\text{Fe}$ bond ($\text{Fe}-\text{C}(1)$ of 1.821 (3) Å) or to the $\text{Fe}-\text{P}$ bond ($\text{Fe}-\text{C}(2)$ of 1.795 (4) Å) presumably due to the poor trans directing influence of a Cl ligand in this environment.

Finally, we note that the experimental value of the $\text{Fe}-\text{P}-\text{Fe}'$ angle (69.8 (0)°) is very close to that predicted ($\sim 70^\circ$) for the halogeno-bridged complexes $\text{Fe}_2(\text{CO})_6(\text{X})(\text{PPh}_2)$ ($\text{X} = \text{Br}$, I) from an analysis of ³¹P NMR shifts for the phosphorus atom in a variety of phosphido-bridged iron complexes.¹

Acknowledgment. We are grateful to the National Research Council of Canada for financial support of this work.

Registry No. $\text{Fe}_2(\text{CO})_6(\text{Cl})(\text{PPh}_2)$, 71000-92-5.

Supplementary Material Available: A listing of structure factor amplitudes and Table SI showing anisotropic thermal parameters (8 pages). Ordering information is given on any current masthead page.

- (9) Matthew, M.; Palenik, G. J.; Carty, A. J.; Paik, H. N. *J. Chem. Soc., Chem. Commun.* **1974**, 25.
 (10) (a) Cotton, F. A.; Johnson, B. F. G. *Inorg. Chem.* **1967**, 6, 2113. (b) Wender, I.; Pino, P. "Organic Synthesis via Metal Carbonyls"; Wiley: New York, 1968; Vol. 1, p 228.

Contribution from the Department of Chemistry,
Howard University, Washington, D.C. 20059

Activation Parameters and a Mechanism for Metal-Porphyrin Formation Reactions

Jafara Turay and Peter Hambright*

Received April 10, 1979

The rates of metal ion incorporation into porphyrins to form metalloporphyrins have been shown to vary with the transition-metal type,¹⁻³ from relatively fast for Cu^{2+} to orders of magnitude slower for Ni^{2+} . Such rates themselves are several million times slower⁴ than those of most conventional metal-ligand substitution processes. With the aim of understanding such differences, we have measured the activation parameters ΔH^\ddagger and ΔS^\ddagger for Cu^{2+} , Zn^{2+} , Co^{2+} , and Ni^{2+} incorporation into tetrakis(*N*-methyl-4-pyridyl)porphyrin in aqueous solution. Similar measurements have been made with porphyrins in acetic acid/water⁵ or DMF⁶ solutions, where the

- (3) "International Tables for X-Ray Crystallography"; Kynoch Press: Birmingham, England, 1974; Vol. IV, p 72.
 (4) Stewart, R. F.; Davidson, E. R.; Simpson, W. T. *J. Chem. Phys.* **1965**, 42, 3175.
 (5) Huntsman, J. R.; Dahl, L. F., unpublished observations quoted in ref 6.
 (6) Clegg, W. *Inorg. Chem.* **1976**, 15, 1609.
 (7) Carty, A. J.; Mott, G. N.; Taylor, N. J.; Yule, J. E. *J. Am. Chem. Soc.* **1978**, 100, 3051.
 (8) Carty, A. J.; Taylor, N. J.; Smith, W. F.; Paik, H. N.; Yule, J. E. *J. Chem. Soc., Chem. Commun.* **1976**, 41.

- (1) F. Longo in "The Porphyrins", Vol. 5, D. Dolphin, Ed., Academic Press, New York, 1978, Chapter 10.
 (2) W. Schneider, *Struct. Bonding (Berlin)*, **23**, 123 (1975).
 (3) P. Hambright in "Porphyrins and Metalloporphyrins", K. M. Smith, Ed., Elsevier, Amsterdam, 1975, Chapter 6.
 (4) R. G. Wilkens, "The Study of Kinetics and Mechanisms of Transition Metal Complexes", Allyn and Bacon, Boston, 1976, Chapter 4.
 (5) E. Choi and E. Fleischer, *Inorg. Chem.*, **2**, 94 (1963).
 (6) F. Longo, E. Brown, D. Quimby, A. Adler, and M. Meot-Ner, *Ann. N.Y. Acad. Sci.*, **206**, 420 (1973).